Low-Temperature Growth of a Nitrogen-Doped Titania Nanoflower Film and Its Ability To Assist Photodegradation of Rhodamine B in Water

ARTICLE *in* THE JOURNAL OF PHYSICAL CHEMISTRY C · OCTOBER 2006

Impact Factor: 4.77 · DOI: 10.1021/jp065630n

2 AUTHORS:

Jin-Ming Wu
Zhejiang University
101 PUBLICATIONS **1,840** CITATIONS

SEE PROFILE

Bin Qi
University of Florida
27 PUBLICATIONS **365** CITATIONS

SEE PROFILE

Low-Temperature Growth of a Nitrogen-Doped Titania Nanoflower Film and Its Ability To Assist Photodegradation of Rhodamine B in Water

Jin-Ming Wu* and Bin Qi

Department of Materials Science & Engineering, Zhejiang University, Hangzhou 310027, People's Republic of China

Received: August 30, 2006; In Final Form: October 13, 2006

Successful application of titania photocatalysts for air and water remediation demands highly active titania thin films fabricated through a simple reaction that is easily scaled-up. In this study, titania thin films with a dual structure, that is, flower-like rutile aggregates sitting on top of an anatase layer, were fabricated simply by oxidizing metallic Ti plates with hydrogen peroxide solution containing trace amounts of hexamethylenetetramine and concentrated nitric acid at 353 K for 72 h. Low-temperature growth of the top flower-like rutile, with constructing blocks of tiny rutile nanorods, occurred only after 60 h of reaction when the solution contained almost no hydrogen peroxide or Ti(IV) ions. Tiny rutile nanorods were supposed to form through a dissolution precipitation mechanism and then orient and attach to form single-crystal nanorods with larger sizes, which self-organize to develop the flower-like rutile aggregates. After a subsequent thermal treatment to further improve the crystallinity, the titania film was utilized to assist photodegradation of Rhodamine B in water under ultraviolet light irradiation. Significant increased photocatalytic activity of the titania nanoflower film was achieved after natural aging of the titania thin film for certain durations. The present film possessed enhanced photocatalytic activity compared with the titania nanorod film we previously reported and the commercial Degussa P-25 titania coating as well.

1. Introduction

Despite the vast research focusing on titania as photocatalysts, there is still a long way to go before bringing this advantageous technique to practical use due mainly to the unsatisfactory photocatalytic activity (PA) as well as the limited ability to utilize solar energy. Titania can be modified to be sensitive to visible light through doping with nonmetallic elements of C and N,[1−5] doping with certain transition-metal ions,[6,7] coupling with semiconductors of band gap narrower than that of titania,[8] or surface sensitizing with certain dyes.[9] To improve the PA of titania, embedding with noble metals such as Pt,[10] Au,[11] and Ag,[12] and also certain kinds of transition-metal ions,[13] to act as electron trap to improve the separation effect of the photogenerated electron−hole pairs is the most commonly adopted tactic (note that negative effects are also reported for the doping of Au and Pt[14]). Because photocatalytic reaction occurs on the surface, titania with an extremely high specific surface area also attracts much attention. For example, mesoporous titania (powders or thin films) with a crystallized wall has been the subject of many studies.[15−17] Titania powders or thin films consisting of nanofeatures of tubes,[18−20] rods,[21−23] whiskers,[24] wires,[25,26] needles,[27] and sheets[28] due partly to the inherent high specific surface area have also been synthesized through various physical, chemical, or electrochemical approaches, most of which involve either templates or annoying reagents and complicated procedures.

Interactions between metallic Ti and hydrogen peroxide are of original interest in the biomaterial fields because Ti is one of the most biocompatible metals and its in vivo oxidation/corrosion behavior as well as its excellent ability to bond firmly with surrounding bone tissue has been related closely to the hydrogen peroxide generated in biological systems.[29−32] Recently, it has been found that porous titania films,[33] titania nanorods,[22,23] and sea-urchin-like spherical aggregates[34] can be synthesized through such a simple reaction. Hexamethylenetetramine (HMT) has been utilized to fabricate nitrogen-doped titania[35−37] and also as a structure-directing agent for fabrication of ZnO[38,39] and CeO_2[40] with certain nanofeatures. Therefore, it is supposed that the addition of certain amounts of HMT in the hydrogen peroxide could lead to the formation of titania with certain nanofeatures and at the same time the realization of nitrogen-doping. In fact, one of the present authors (J.-M.Wu) has successfully synthesized titania thin films with flower-like top layers through reactions of metallic titanium with hydrogen peroxide solutions containing HMT and certain concentrated nitric acids. The preliminary results revealed ideal PA of the achieved titania film.[41] In this study, the low-temperature growth of such nitrogen-doped crystallized titania thin films with flower-like top layers were examined in detail and the ability of the thin films to assist photodegradation of Rhodamine B (RhB) in water was evaluated. It is believed that the fabrication of the titania thin film with high PA through a simple reaction that is easily scaled-up should contribute to the future application of titania photocatalysts for air and water remediation.

2. Experimental Section

2.1. Sample Preparation. Titanium plates of dimensions 5 × 5 × 0.01 cm^3 were etched at ambient temperature for 2 min in a 1:3:6 (by volume) mixture of concentrated hydrofluoric acid, concentrated nitric acid, and distilled water. They were then cleaned in an ultrasonic bath. Each Ti plate was immersed in 50 mL of 30 mass % H_2O_2 solution which contained 100 mg of HMT and 1.0 mL of concentrated nitric acid and kept

* To whom correspondence should be addressed. Phone: +86-571-87953115. Fax: +86-571-87952358. E-mail: msewjm@zju.edu.cn.

10.1021/jp065630n CCC: $37.00
Published on Web 12/14/2006

for up to 72 h in an oven maintained at 80 °C. The surface-oxidized Ti was then rinsed gently in distilled water and dried for further characterization. Heat treatment was conducted in air at 450 °C for 1 h.

Nanoparticles of commercial Degussa P-25 TiO_2 (a mixture of anatase and rutile, with an average particle size of 30 nm and BET surface area of 50 m^2/g) were deposited on the pretreated Ti plates by repeatedly dipping them in the P-25 ethanolic suspension (25 g/L) and drying them in air at 105 °C to obtain a film mass of ca. 0.9 mg/cm^2.

2.2. Characterization. The Ti(IV) concentration was measured with inductively coupled plasma (ICP) atomic-emission spectroscopy (IRIS Intrepid II XSP, Thermostat, USA). The hydrogen peroxide concentration was determined by titration using standard potassium permanganate solution. The X-ray diffraction (XRD) measurements were conducted on a Rigaku D/max 2550PC diffractometer with Cu Kα radiation, operated at 40 kV and 300 mA (λ = 0.154056 nm). The surface morphology was observed using field emission scanning electron microscopy (FE-SEM; Sirion 100, FEI). Transmission electron microscopy (TEM) observations were conducted employing a JEM-200CX microscope (JEOL, Japan) working at 160 kV. To prepare the sample for TEM characterization, the Ti plate after 72 h of reaction was soaked in ethanol and subjected to strong ultrasonic vibrations to detach the surface powders, which were then placed on a carbon-precoated copper grid. The X-ray photoelectron spectroscopy (XPS) spectra were measured using an ESCA spectrometer (S-Probe ESCA SSX-100S, Fisons Instrument) and monochromatized Al Kα X-ray (1486.8 eV) irradiation. The binding energy was normalized to the C 1s energy (284.46 eV) for adventitious hydrocarbons as the indirect standard. UV−vis diffuse reflectance spectra of titania films were collected using a UV−vis near-infrared spectrometer (UV-3150, Shimadzu, Japan). Raman spectral analysis was conducted using an Almega dispersive Raman system (Nicolet) and a Nd:YAG intracavity doubled laser operating at 532 nm with an incident power of 10 mW. Nitrogen sorption measurements were conducted at 77 K using Autosorb-1 (Quantachrome Instruments) on powders scratched from the Ti plate after reaction with the H_2O_2 solution at 80 °C for 72 h, followed by heating in air at 450 °C for 1 h. The Brunauer−Emmett−Teller (BET) approach using adsorption data over the relative pressure ranging from 0.06 to 0.26 was utilized to determine the specific surface area. The sample was degassed at 150 °C to remove physisorbed gases prior to the measurement.

2.3. Photocatalytic Activity Evaluation. The PA was measured using RhB aqueous solution as a probe in a pyrex reactor with a water jacket. A 50 mL sample of RhB solution with an initial concentration of 0.005 mM in the presence of the titania films (2.5 × 2.5 cm^2) was illuminated with a 450 W high-pressure mercury lamp 6 cm above the solution. The average intensity of UV irradiance reaching the samples was measured to be ca. 1.4 mW/cm^2, using a UV irradiance meter (model UV-A, Beijing Normal University, China, measured for the wavelength range of 320−400 nm with a peak wavelength of 365 nm). The solution was stirred continuously by a magnetic stirrer and exposed to air during the photocatalytic reaction. The solution temperature was maintained at around 30 °C using a water-cooling system. The change in RhB concentration was monitored using a 752 UV−vis spectrophotometer at a wavelength of 555 nm, with a quartz cuvette of 1 cm optical path length.

3. Results

3.1. Time Dependence of the Reaction. Hydrogen peroxide hardly decomposes at 80 °C; however, in presence of Ti(IV) ions, its decomposition rate accelerates due to the catalytic effect of the transition-metal ions, which produces strong oxidative radicals, leading to the formation of amorphous titania gel on the surface of the Ti plate. Figure 1 shows the concentration of H_2O_2 molecules and the Ti(IV) ions in the solution as a function of the reaction time. Those measured in the 30 mass % H_2O_2 solution, that is, without the additives of HMT and nitric acid in the solution, are given as references. In both cases, the H_2O_2 decomposed almost linearly with the reaction time. Combined addition of HMT and nitric acid in the solution retarded the decomposition of the H_2O_2 molecules. Without the additives, H_2O_2 decomposed within 12 h, while for the solution containing HMT and nitric acid, 10 mass % H_2O_2 still remained, which decomposed only after a prolonged reaction time of 24 h. Accordingly, fewer Ti(IV) ions were detected in the solution with the additives. After 1 h of reaction, the amounts of Ti(IV) ions reached their maximum of 5.8 and 11.2 mM, respectively, in the cases with and without the additives in the solution.

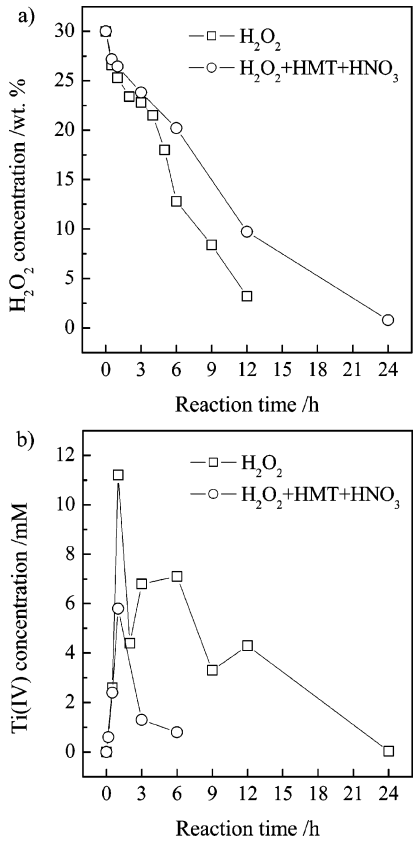

Figure 1. Dependence of the H_2O_2 (a) and Ti(IV) ion (b) concentrations on the duration of the reaction at 80 °C between Ti and 30 wt % H_2O_2 and that containing 0.014 M HMT and 0.2 M HNO_3.

Changes in the surface morphology of the Ti plate after reaction for various durations are illustrated in Figure 2. A condensed amorphous titania layer covered the Ti surface after 10 min of reaction (Figure 2a). After only 1 h, a porous titania layer with an average pore size of ca. 70 nm developed (Figure 2b). Figure 2c shows that the surface pores grew to hundreds of nanometers with a prolonged reaction time of 12 h. The wall thickness also increased with the prolonged reaction time, and the titania grew to give a palplike morphology as evident after 48 h of reaction (Figure 2d). Flower-like titania appeared on the surface only after 60 h of reaction (Figure 2e). The film achieved after 72 h of reaction also exhibited such flower-like aggregates and will be characterized in detail later.

For reaction durations of 6−60 h, a different flower-like titania aggregate was also found. Figure 3 shows the typical

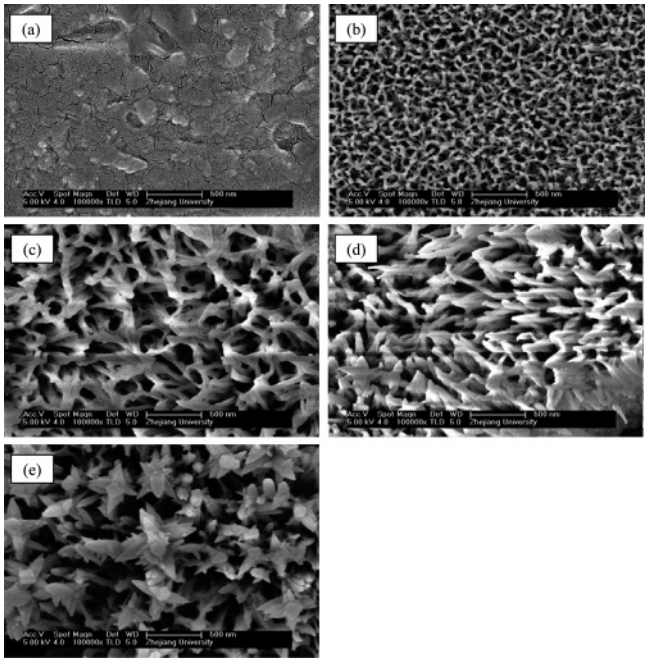

Figure 2. FE-SEM morphologies of titania films obtained by oxidizing Ti with 30 mass % H_2O_2 solutions containing 0.014 M HMT and 0.2 M HNO_3 at 80 °C for (a) 10 min, (b) 1 h, (c) 12 h, (d) 48 h, and (e) 60 h.

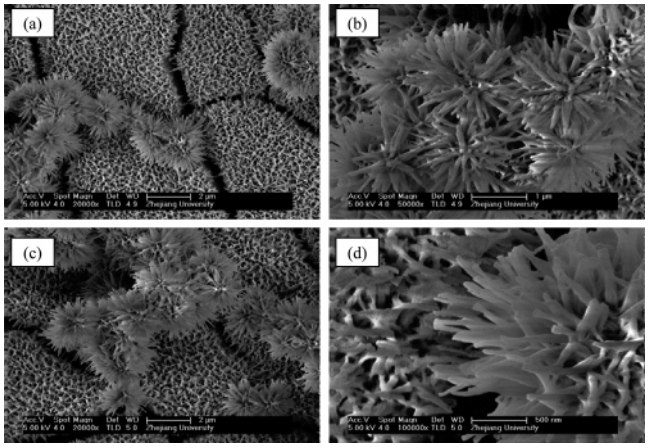

Figure 3. FE-SEM morphologies of titania films obtained by oxidizing Ti with 30 mass % H_2O_2 solutions containing 0.014 M HMT and 0.2 M HNO_3 at 80 °C for (a, b) 6 h and (c, d) 12 h, showing flower-like aggregates precipitated from the solution.

morphologies obtained after 6 and 12 h of reaction. Each titania aggregate was ca. 2 μm in diameter. High-magnification images indicate that the flower-like aggregate consisted of titania nanorods with sizes of ca. 60 nm diameter and 580 nm length, which grew outside from a center point to give roughly a spherelike outline.

Figure 4a illustrates the XRD patterns of the titania film obtained with various reaction durations. Within 48 h of reaction, mainly amorphous titania was detected. After 60 h of reaction, except the peaks corresponding to the Ti substrate, minor peaks corresponding to anatase and rutile were discernible. The intensity of these peaks increased significantly with a prolonged reaction time of 72 h. Note the distinct full width at half-maximum (fwhm) for the strongest peaks corresponding to anatase (101), located at $2\theta = 25.3°$, and rutile (110), located at $2\theta = 27.5°$. A rough estimation of the grain size using the Scherrer formula obtained values of 9.2 nm for anatase and 25.6 nm for rutile.[32] After a subsequent heat treatment at 450 °C

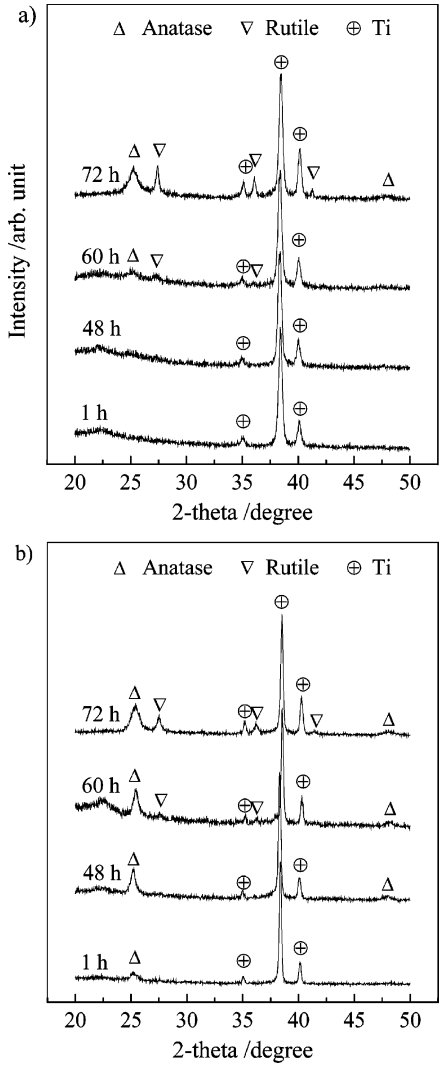

Figure 4. XRD patterns of titania films obtained by oxidizing Ti with 30 mass % H_2O_2 solutions containing 0.014 M HMT and 0.2 M HNO_3 at 80 °C for various durations (a), followed by heating in air at 450 °C for 1 h (b).

for 1 h in air, the amorphous titania crystallized to give anatase peaks in the corresponding XRD spectra, as shown in Figure 4b.

The relative weight percentage of the rutile phase, W_R, can be estimated according to the formula[32]

$$W_R = 1/(1 + 0.8I_A/I_R) \quad (1)$$

where I_A and I_R are the X-ray integrated intensities of the (101) reflections of anatase and (110) reflections of rutile, respectively. After the subsequent thermal treatment, W_R for the titania film obtained by 72 h of reaction decreased from the as-deposited 58% to 42%, due to the crystallization of the sublayer amorphous titania mainly to the anatase phase (will be shown in Figure 7 later).

3.2. Titania Nanoflower Film. Figure 5 shows the FE-SEM morphology of the titania film obtained by 72 h of reaction. An overall view in Figure 5a illustrates the many flower-like titania aggregates sitting on top of the porous titania layer. There are also regions no such flower-like aggregates can be found, especially near the microcracks of the porous titania sublayer. A closer examination indicates that the flower-like titania aggregates are aligned in various directions (Figure 5b). The high-magnification image in Figure 5c discloses that the exact

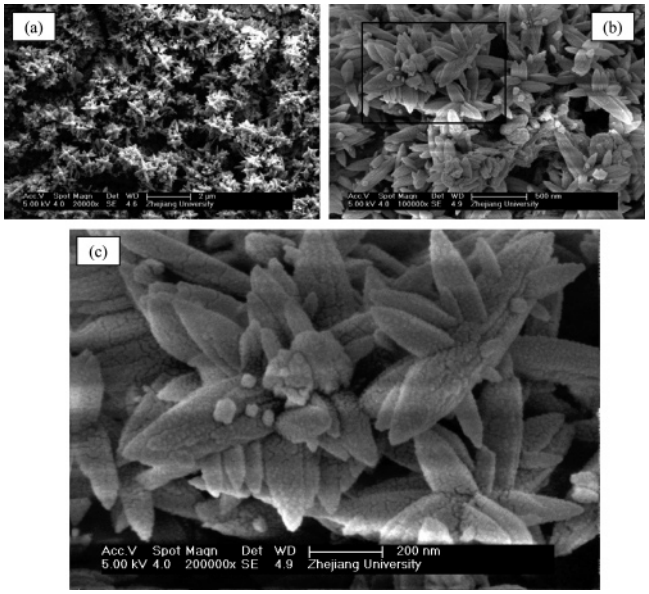

Figure 5. FE-SEM morphologies of titania films obtained by oxidizing Ti with 30 mass % H_2O_2 solutions containing 0.014 M HMT and 0.2 M HNO_3 at 80 °C for 72 h. A high magnification of the marked region in (b) is shown as (c).

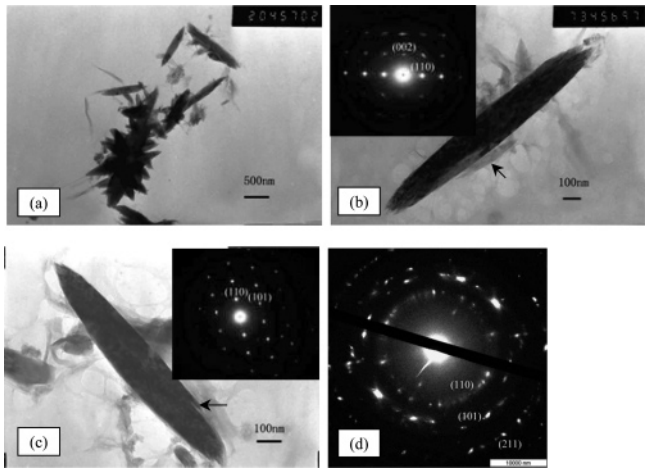

Figure 6. TEM images of the titania nanoflowers (a) and their constructing blocks of spindle-like nanorods together with the corresponding SAD patterns as insets (b, c). The SAD pattern shown in (d) illustrates that the titania nanoflower as a whole consisted also of pure rutile.

morphology of a single titania aggregate is some tiny titania nanorods growing outside from different sites of a main trunk which was 180 nm in diameter and 700 nm in length. Both sides of the main trunk and the outside of the branches were cuspidal. For simplicity, we call titania aggregates with such morphology a "titania nanoflower" and the titania film achieved by 72 h of reaction a "titania nanoflower film" hereafter. Various alignments of the titania nanoflower gave different morphologies when viewed from the very top. It is noted that, without the additives of HMT and concentrated nitric acid in the solution, the reaction led to a titania film with well-aligned titania nanorods in the top layer, which we call a "titania nanorod film" and which has been reported previously.[22,23]

The TEM image of a titania nanoflower is demonstrated in Figure 6a. The selection area diffraction (SAD) pattern of an isolated titania nanorod suggests that the nanorod was single-crystal rutile. A close examination reveals that the nanorod consisted of a few well-aligned tiny nanorods fused with each other, as indicated with arrows in Figure 6b,c. The SAD pattern

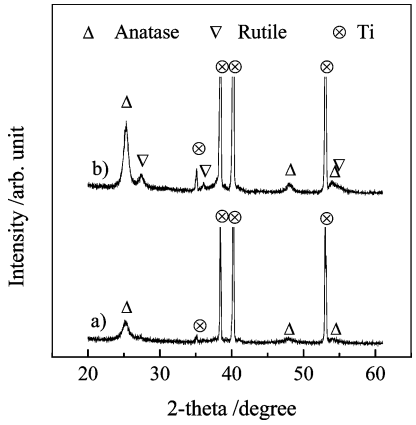

Figure 7. XRD patterns of the titania nanoflower film after ultrasonic cleaning to remove the top nanoflower layer (a), followed by heating in air at 450 °C for 1 h (b).

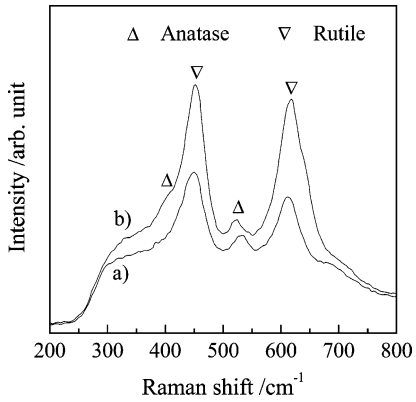

Figure 8. Raman spectra of the titania nanoflower film obtained by oxidizing Ti with 30 mass % H_2O_2 solutions containing 0.014 M HMT and 0.2 M HNO_3 (a), followed by heating in air at 450 °C for 1 h (b).

collected from several titania nanoflowers gave discrete rings corresponding to pure rutile (Figure 6d); therefore, it can be concluded that the large nanorods formed through an "oriented attachment" mechanism which was developed first by Penn et al.[42] Because the growing directions of the single-crystal rutile varied from nanorod to nanorod (Figure 6b,c), the rutile nanoflower film as a whole exhibited an XRD pattern characteristic of multicrystal rutile and gave no remarkable hints of oriented growth, which was evident for the titania nanorod film.[23]

Since most of the nanorods constructing the titania nanoflower were identified to be pure rutile, it is very likely that the anatase detected in the XRD pattern shown in Figure 4 came from the layer below the titania nanoflower. Therefore, the top nanoflower layer was removed by a strong ultrasonic vibration, and the remaining layer was subjected to XRD characterization. Figure 7 shows that the porous titania layer below the nanoflower was pure anatase (curve a). After the subsequent thermal treatment, the XRD intensity corresponding to anatase increased and some peaks corresponding to rutile appeared (curve b). The rutile (110) peak in curve b exhibited a much increased fwhm as compared to those found in Figure 4a (72 h). Therefore, the minor rutile phase found in curve b of Figure 7 resulted from crystallization of the amorphous titania, rather than the possibly remaining rutile nanoflower aggregates.

Figure 8 shows the Raman spectra of the titania nanoflower film achieved by 72 h of reaction, before and after the subsequent thermal treatment. The peaks located at 400 and 527 cm^{-1} can be ascribed to anatase,[22] and the two peaks located at 452

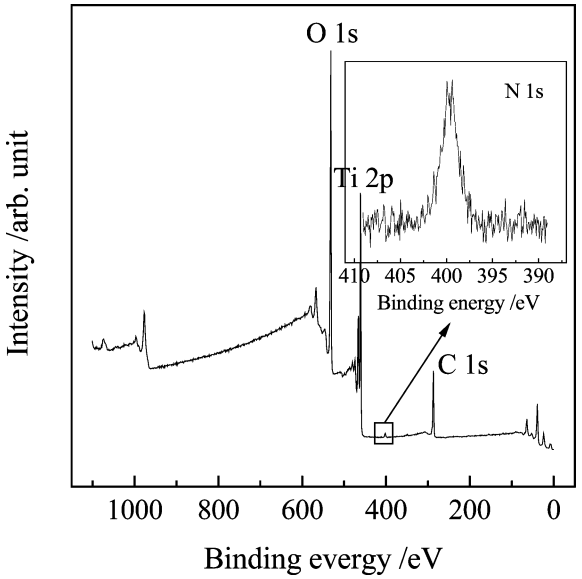

Figure 9. Wide-scan X-ray photoelectron spectrum of the titania nanoflower film obtained by oxidizing Ti with 30 mass % H_2O_2 solutions containing 0.014 M HMT and 0.2 M HNO_3, followed by heating in air at 450 °C for 1 h. The inset is the X-ray photoelectron spectrum of the N1s core level.

and 618 cm^{-1} correspond to rutile.[22] Thus, it is further confirmed that the titania nanoflower film as a whole was a mixture of anatase and rutile. Significantly stronger peaks can be discerned after the titania layer is heated in air at 450 °C for 1 h, which can be ascribed to the greater concentrations of the crystalline titania phase;[43] therefore, the subsequent calcination improved significantly the crystallinity of the low-temperature derived titania nanoflower film, which can also be discerned from the XRD results shown in Figure 7. It is noted that, although there were significant amounts of anatase in the titania nanoflower film, the Raman peaks corresponding to anatase were quite weak. This can be ascribed to the fact that the top layer of the film consisted mainly of pure rutile nanoflowers. During the Raman spectrum test, such a rough top layer inhibited the penetration of the exciting laser to the sublayer of anatase, and hence, less excited signals corresponding to anatase were detected.

Figure 9 shows the XPS spectrum of the titania nanoflower film. A broad peak in the region of 396−403 eV, with a maximum located at the bonding energy of 399.6 eV, was identified clearly, which could be contributed to N1s. A similar peak located at the bonding energy near 399.6 eV has also been identified by Diwald[44] and Gao et al.[45] from their ammonia-treated titania and has been ascribed to a form of nitrogen that is probably bound to hydrogen[44] or hyponitrite.[45] The amounts of nitrogen in the titania nanoflower film were determined to be ca. 1.4 atom %.

Figure 10gives the UV−vis reflectance spectrum of the titania nanoflower film. That of the titania nanorod film is given as a reference. Both films adsorbed light with a wavelength below 415 nm. The reflectance for the titania nanoflower film was remarkably higher than that of the titania nanorod film, which could be contributed to the randomly aligned nanoflowers on the surface, causing more reflectance of the light. No remarkable absorbance of visible light, which has been anticipated for the nitrogen-doped titania, can be discerned for the present nitrogen-doped titania nanoflower film.

The BET specific surface area of the powders scratched from the thermally treated titania nanoflower film was measured to be 77.8 m^2/g using N_2 adsorption at 77 K. It is noted that the surface area of titania powders derived by a sol−gel procedure, which were also a mixture of anatase and rutile, was reduced from the as-prepared 153 to 23 m^2/g after calcination at 500 °C for 2 h.[46] It seems that the unique nanostructure achieved in the current investigation favors maintaining a high specific surface area upon subsequent thermal treatment.

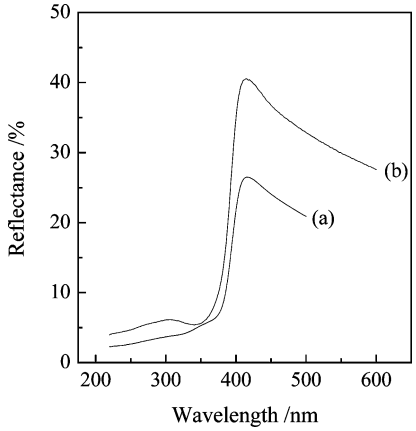

Figure 10. UV−vis reflectance spectra of the titania films obtained by oxidizing Ti at 80 °C for 72 h with 30 mass % H_2O_2 solution (a) and that containing 0.014 M HMT and 0.2 M HNO_3 (b).

3.3. Photocatalytic Tests. After preservation of the titania thin films at ambient conditions for certain durations, a gradual but significantly enhanced ability of titania to assist photodegradation of RhB in water, which we call natural aging, has been noticed recently and will be published elsewhere.[47] Therefore, photodegradation of RhB in the presence of the titania nanoflower film after the film was heated at 450 °C for 1 h followed by preservation at ambient conditions for 0, 10, 20, and 30 d was tested, and the results are shown in Figure 11a. Figure 11b shows the relationship between $\ln(c_0/c)$ and the irradiation time t. As all the curves can be fitted roughly to a straight line, the photocatalytic degradation reaction can be assumed to follow a pseudo-first-order expression[48]

$$\ln(c_0/c) = kt \tag{2}$$

where c/c_0 is the normalized RhB concentration and k is the apparent reaction rate (min^{-1}). Figure 12 illustrates the corresponding pseudo-first-order reaction rate constants (k) as a function of the preservation time. As expected, the rate constant increased from the as-heated 0.53×10^{-2} to 1.79×10^{-2} min^{-1} after 10 d of aging and increased gradually further with prolonged aging time.

The PA of the titania nanoflower film was compared to that of the titania nanorod film as well as the titania coating prepared by casting from a Degussa P25 slurry. Figure 12 shows that, for a rough comparison, the PA of the titania nanoflower film was almost triple that of the P25 coating after natural aging for 10 d. In addition, the present titania nanoflower film also exhibits an advantageous ability to assist photodegradation of RhB over the titania nanorod film, which has been identified to possess excellent PA.[23]

4. Discussion

4.1. Formation of the Rutile Nanoflower. Surface oxidation of Ti with H_2O_2 leads to a porous layer of hydrated titanium oxide, which has been identified to be $Ti^{4+}(OH^-)_2O_2^{2-}-Ti^{4+}(OH^-)_2O_2^{-}-Ti^{4+}(OH)_x-TiO_2 \cdot nH_2O$.[29] In the present reaction, for the first 10 min, the reaction was believed to proceed through

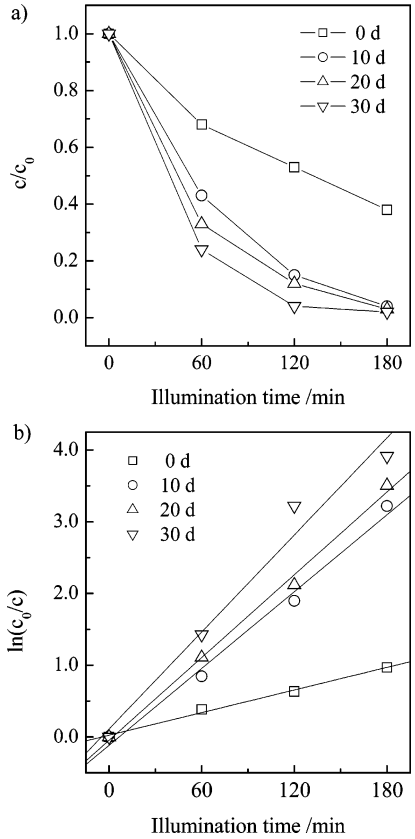

Figure 11. Photodegradation curves of RhB assisted with the titania nanoflower film subjected to heating in air at 450 °C for 1 h followed by natural aging for various durations (a). The fitting results using the pseudo-first-order reaction are shown in (b).

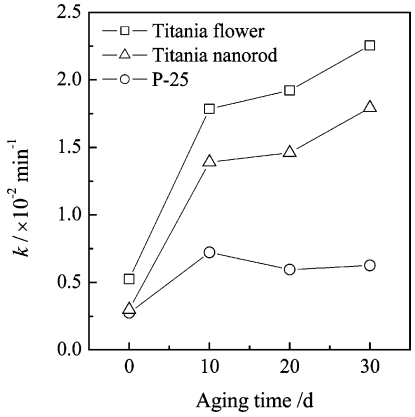

Figure 12. Apparent reaction rate constant for the titania nanoflower film as a function of the natural aging time. Those for the titania nanorod film and commercial Degussa P-25 film are also shown as references.

mainly out-diffusion of the Ti species to react with H_2O_2 at the oxide/solution interface.[49] Because of the very thin oxide film formed at the beginning of the reaction, the nucleation rate of hydrated titanium oxide was high, which thus resulted in a relatively condensed thin layer as shown in Figure 2a. After a critical thickness of the oxide was obtained, the oxidation kinetics changed, which proceeded mainly through the diffusion of H_2O_2 through the oxide layer to react with Ti at the Ti/oxide interface.[49] Such subsequent reaction with a significantly reduced rate led to a porous oxide layer on the surface, and the pore size increased with increasing oxide film thickness, which is in agreement with the results of DeRosa et al.[49]

The oxidation rate in the second stage was controlled by the diffusion rate of H_2O_2 molecules through the oxide layer. At a temperature of 80 °C, HMT decomposed gradually through the following reaction:[39,41]

$$(CH_2)_6N_4 + 6H_2O + 4H^+ \rightleftharpoons 6HCHO\uparrow + 4NH_4^+ \quad (3)$$

The resulting ammonia ions, as well as the nitrate ions in the solution, were supposed to incorporate into the hydrated oxide layer, which inhibited the diffusion of the H_2O_2 molecules and hence decelerated the decomposition rate of the H_2O_2 molecules, as illustrated in Figure 1a. It is noted that, without the additive of nitric acid to compensate the increasing pH value in the solution due to eq 3, H_2O_2 decomposed rapidly, leading to no remarkable formation of titanium oxide on the Ti surface.

A decrease in the Ti(IV) concentration in the solution after 1 h of reaction suggested precipitation of titania. Thus, the Ti(IV) concentration demonstrated in Figure 1b was a dynamic balance between attack of metallic Ti by H_2O_2, dissolution of the formed hydrated titania, and precipitation of titania back onto the Ti surface or in the solution.

The rutile nanoflower appeared on the Ti surface only after 60 h of reaction (Figure 2), at which stage the H_2O_2 was consumed thoroughly and the dynamic Ti(IV) concentration was very low (Figure 1). Therefore, it is believed that, after 60 h of reaction, the previously formed hydrated amorphous titania dissolved in the acidic solution, and then the rutile nanoflower precipitated due to the supersaturated Ti(IV) solution in thermodynamics. Two factors were believed to contribute to the low-temperature growth of the rutile nanoflower: the additives of HMT and nitric acid and the porous hydrated titania layer formed before 60 h of reaction.

Without the present additives in the H_2O_2 solution, a top layer of well-aligned titania nanorods (a mixture of anatase and rutile) was obtained on the Ti surface.[22] Therefore, in the present reaction, the ammonia and nitrate ions in the solution contributed to the formation of the titania nanoflower, probably through being adsorbed in certain planes of the precipitated titania, which directed the growth of titania to form the present flower-like morphology. The same effect of HMT on the growth of the ZnO nanoflower has also been reported.[39]

To study the possible effect of the substrate on the low-temperature growth of the rutile nanoflower, the present reaction was interrupted at intervals of 24, 48, 52, 56, and 60 h, and a Ti substrate pretreated with 30 mass % H_2O_2 solution at 80 °C for 10 min was used to replace the original Ti plate. A monolayer of well-aligned rutile nanorods, instead of the present nanoflower, was obtained on the pretreated Ti surface.[50] Therefore, the porous hydrated titania layer formed before 60 h of reaction was believed to guide the growth of the present rutile nanoflower.

The TEM observation in Figure 6 suggests that the formation mechanism of the rutile nanorods, which were the constructing blocks for the present rutile nanoflower, was very similar to that reported by Li et al.[51] After the Ti(IV) ions dissolved from the previously formed hydrated amorphous titania accumulated to a critical concentration, tiny rutile nanorods precipitated. Such tiny rutile nanorods aligned to form a bundle of independent nanorods which coalesced and fused with each other to form a single larger nanorod, driven by the reduced interfacial energy.[42] The self-assembly procedure of the large nanorod to form a nanoflower is not clear at the present time; however, the fact that the nucleation and growth of the nanorod from a main trunk demands less nucleating energy and a relatively lower supersaturation of the Ti(IV) solution with respect to titania should favor the formation of such flower-like aggregates.

Although XRD peaks corresponding to crystallized anatase were detected for the thin film obtained after 60 h of the present reaction (Figure 4), a significant amount of the sublayer titania still remained amorphous, which crystallized mainly to anatase after a subsequent thermal treatment (Figure 7). Therefore, the subsequent thermal treatment contributes to not only the adhesion of the rutile nanoflower to the Ti substrate, but also the improved crystallinity, both of which play positive roles for titania films as photocatalysts.

4.2. Photocatalytic Activity of the Titania Nanoflower Film. It turns out that, under the irradiation of the high-pressure mercury lamp, the decomposition of RhB, without the assistance of the titania, is ignorable.[23,48] In the presence of the titania, the photodecomposition of RhB proceeds in both the photocatalytic pathway and the photosensitization pathway, both of which are dependent on the PA of the titania.[48,52] The titania nanoflower film synthesized in the current investigation exhibited higher PA than the titania coating derived from the commercial Degussa P25 slurry and also the titania nanorod film we fabricated previously.[23] Note that here the comparison of PA for the three films only gives a hint of how active the present titania nanoflower film could be, because many factors readily affecting the PA, such as the morphology, particle size, and crystal phase,[53] for the three films varied significantly, and hence, exact analysis of the causes of the difference in PA for the three films is not possible and at the same time meaningless.

The top layer of the present titania nanoflower film was identified to be pure rutile, which has been found to possess poorer PA than anatase because of its poor activity for the reduction of oxygen,[54] which acts as an electron acceptor in most photocatalytic reactions including the present one.[48] This fact emphasizes the contributions of the unique morphology of nanoflowers to the PA, which possessed a high specific surface area of ca. 77.8 m^2/g after the thermal treatment. In addition, there were significant gaps in the rutile nanoflower layer; therefore, the anatase film underneath also contributed positively to the PA. It is noted that the presence of a small amount of an anatase component is crucial for an efficient photocatalytic reaction on TiO_2 particles using oxygen as the electron acceptor.[54]

Doping of nitrogen has been well accepted to enhance the PA of titania under visible light illumination, although the exact mechanism is still a controversial topic.[45] In addition, there are contrary reports concerning the effects on the visible light activity of the incorporated nitrogen in titania, which gives a peak of ca. 399.6 eV in XPS spectra. Gao et al. argued that it is unlikely for such nitrogen to be responsible for the visible light response,[45] while Diwald et al. found that nitrogen with a N1s binding energy of 399.6 eV is effective in reducing the threshold photon energy for titania from 3.0 to 2.4 eV, which is a shift of 0.6 eV into the visible spectral region.[44] In the current investigation, although a significant N1s peak with a binding energy of 399.6 eV was also identified (Figure 9), the adsorption threshold of the titania nanoflower film was almost the same as that of the titania nanorod film synthesized using the H_2O_2 solution containing no nitrogen sources (Figure 10). It is thus unlikely for the incorporated nitrogen to contribute significantly to the achieved high PA under the present testing conditions.

5. Conclusions

A dual-structure titania thin film was synthesized by direct oxidation of titanium substrates with hydrogen peroxide solutions containing HMT and concentrated nitric acid at 80 °C for 72 h. Before 60 h of reaction, a porous hydrated titania layer was deposited onto the titanium substrates, on which a top layer of rutile nanoflowers precipitated with a prolonged reaction time of up to 72 h. During the reaction period from 60 to 72 h, tiny rutile nanorods precipitated from the solution, which aligned to form a bundle and eventually fused through an "oriented attachment" mechanism to achieve a larger nanorod. The large nanorod self-assembled to give a flower-like morphology, with the help of structure-directing agents of ammonia and nitrate ions in the solution. The porous amorphous titania layer underneath, which crystallized mainly to anatase through a subsequent thermal treatment, contributed to the formation of the top low-temperature-crystallized rutile nanoflower layer.

The structure-directing agent of HMT helped not only the formation of the rutile nanoflower aggregates, but also the synchronal incorporation of nitrogen into the titania. However, the incorporated nitrogen, which gives a peak with an N1s binding energy of 399.6 eV, induced no remarkable red shift for the light response of the titania nanoflower film. The excellent photocatalytic ability of the present titania nanoflower film to assist photodegradation of Rhodamine B in water was ascribed predominantly to its unique morphology of the top layer.

Acknowledgment. This work was supported by the National Natural Science Foundation of China (Project No. 50502029).

References and Notes

(1) Khan, S. U. M.; Al-Shahry, M.; Ingler, W. B., Jr. *Science* **2002**, *297*, 2243.
(2) Asahi, R.; Morikawa, T.; Ohwaki, T.; Aoki, K.; Taga, Y. *Science* **2001**, *293*, 269.
(3) Burda, C.; Lou, Y. B.; Chen, X. B.; Samia, A. C. S.; Sout, J.; Gole, J. L. *Nano Lett.* **2003**, *3*, 1049.
(4) Gole, J. L.; Stout, D.; Burda, C.; Lou, Y. B.; Chen, X. B. *J. Phys. Chem. B* **2004**, *108*, 1230.
(5) Oliver, D.; Thompson, T. L.; Zubkov, T.; Goralski, E. G.; Walck, S. D.; Yates, J. T., Jr. *J. Phys. Chem. B* **2004**, *108*, 6004.
(6) Klosek, S.; Raftery, D. *J. Phys. Chem. B* **2001**, *105*, 2815.
(7) Kato, H.; Kudo, A. *J. Phys. Chem. B* **2002**, *106*, 5029.
(8) Ho, W.; Yu, J. C.; Lin, J.; Yu, J.; Li, P. *Langmuir* **2004**, *20*, 5865.
(9) Tachibana, Y.; Haque, S. A.; Mercer, I. P.; Moser, J. E.; Klug, D.; Durrant, J. R. *J. Phys. Chem. B* **2001**, *105*, 7424.
(10) Ryu, J. H.; Choi, W. Y. *Environ. Sci. Technol.* **2004**, *38*, 2928.
(11) Ohtani, B.; Nishimoto, S. *J. Phys. Chem.* **1993**, *97*, 920.
(12) Chandrasekharan, N.; Kamat, P. V. *J. Phys. Chem. B* **2000**, *104*, 10851.
(13) Paola, A. D.; Marci, G.; Palmisano, L.; Schiavello, M.; Uosaki, K.; Ikeda, S.; Ohtani, B. *J. Phys. Chem. B* **2002**, *106*, 637.
(14) Haick, H.; Paz, Y. *J. Phys. Chem. B* **2003**, *107*, 2319.
(15) Zhou, Y.; Antonietti, M. *J. Am. Chem. Soc.* **2003**, *125*, 14960.
(16) Ma, T.; Akiyama, M.; Abe, E.; Imai, I. *Nano Lett.* **2006**, *5*, 2543.
(17) Zhang, Y.; Li, J.; Wang, J. *Chem. Mater.* **2006**, *18*, 2917.
(18) Imai, H.; Takei, Y.; Shimizu, K.; Matsuda, M.; Hirashima, H. *J. Mater. Chem.* **1999**, *9*, 2971.
(19) Tian, Z. R.; Voigt, J. A.; Liu, J.; Mckenzie, B.; Xu, H. F. *J. Am. Chem. Soc.* **2003**, *125*, 12384.
(20) Varghese, O. K.; Gong, D.; Paulose, M.; Ong, K. G.; Dickey, E. C.; Grimes, C. A. *Adv. Mater.* **2003**, *15*, 624.
(21) Limmer, S. J.; Chou, T. P.; Cao, G. Z. *J. Mater. Sci.* **2004**, *39*, 895.
(22) Wu, J. M. *J. Cryst. Growth* **2004**, *269*, 347.
(23) Wu, J. M.; Zhang, T. W.; Zeng, Y. W.; Satoshi, H.; Tsuru, K.; Osaka, A. *Langmuir* **2005**, *21*, 6995.
(24) Zhu, Y. C.; Li, H. L.; Koltypin, Y.; Hacohen, Y. R.; Gedanken, A. *Chem. Commun.* **2001**, *24*, 2616.
(25) Miao, Z.; Xu, D. S.; Ouyang, J. H.; Guo, G. L.; Zhao, X. S.; Tang, Y. Q. *Nano Lett.* **2002**, *2*, 717.
(26) Wu, J. M.; Shih, H. C.; Wu, W. T.; Tseng, Y. K.; Chen, I. C. *J. Cryst. Growth* **2005**, *281*, 384.
(27) Weng, C. C.; Hsu, K. F.; Wei, K. H. *Chem. Mater.* **2004**, *16*, 4080.
(28) Skai, N.; Ebina, Y.; Takada, K.; Sasaki, T. *J. Am. Chem. Soc.* **2004**, *126*, 5851.

(29) Tengvall, P.; Elwing, H.; Lundstrom, I. *J. Colloid Interface Sci.* **1989**, *130*, 405.
(30) Pan, J.; Thierry, D.; Leygraf, C. *Electrochim. Acta* **1996**, *41*, 1143.
(31) Ohtsuki, C.; Iida, H.; Hayakawa, S.; Osaka, A. *J. Biomed. Mater. Res.* **1997**, *35*, 39.
(32) Wu, J. M.; Satoshi, H.; Tsuru, K.; Osaka, A. *J. Am. Ceram. Soc.* **2004**, *87*, 1635.
(33) Wu, J. M.; Satoshi, H.; Tsuru, K.; Osaka, A. *Scr. Mater.* **2002**, *46*, 101.
(34) Mao, Y. B.; Kanungo, M.; Hemraj-Benny, T.; Wong, S. S. *J. Phys. Chem. B* **2006**, *110*, 702.
(35) Nagaveni, K.; Hegde, M. S.; Ravishankar, N.; Subbanna, G. N.; Madras, G. *Langmuir* **2004**, *20*, 2900.
(36) Yin, S.; Yamaki, H.; Komats, M.; Zhang, Q. W.; Wang, J. S.; Tang, Q.; Saito, F.; Sato, T. *J. Mater. Chem.* **2003**, *13*, 2996.
(37) Yin, S.; Zhang, Q. W.; Saito, F.; Sato, T. *Chem. Lett.* **2003**, *32*, 358.
(38) Gao, X. D.; Li, X. M.; Yu, W. D. *J. Solid State Chem.* **2005**, *178*, 1139.
(39) Yin, S.; Sato, T. *J. Mater. Chem.* **2005**, *15*, 4584.
(40) Zhang, F.; Jin, Q.; Chan, S. W. *J. Appl. Phys.* **2004**, *95*, 4319.
(41) Wu, J. M.; Huang, B.; Wang, M.; Osaka, A. *J. Am. Ceram. Soc.* **2006**, *89*, 2660.
(42) Penn, R. L.; Banfield, J. F. *Science* **1998**, *281*, 969.
(43) Lottici, P. P.; Bersani, D.; Braghini, M.; Montenero, A. *J. Mater. Sci.* **1993**, *28*, 177.
(44) Diwald, O.; Thompson, T. L.; Goralski, E. G.; Walck, S. D.; Yates, J. T., Jr. *J. Phys. Chem. B* **2004**, *108*, 6004.
(45) Gao, B. F.; Ma, Y.; Cao, Y. A.; Yang, W. S.; Yao, J. N. *J. Phys. Chem. B* **2006**, *110*, 14391.
(46) Yao, B. D.; Zhang, Y.; Shi, H. Z.; Zhang, L. D. *Chem. Mater.* **2000**, *12*, 3740.
(47) Wu, J. M.; Huang, B. Enhanced Ability of Nanostructured Titania Film to Assist Photodegradation of Rhodamine B in Water through Natural Ageing. *J. Am. Ceram. Soc.*, in press.
(48) Wu, J. M.; Zhang, T. W. *J. Photochem. Photobiol., A* **2004**, *162*, 171.
(49) DeRosa, D. M.; Zuruzi, A. S.; MacDonald, N. C. *Adv. Eng. Mater.* **2006**, *8*, 77.
(50) Wu, J. M.; Qi, B. Low-temperature Growth of Monolayer Rutile TiO_2 Nanorod Film. *J. Am. Ceram. Soc.*, in press.
(51) Li, Q. C.; Kumar, V.; Li, Y.; Zhang, H. T.; Marks, T. J.; Chang, R. P. H. *Chem. Mater.* **2005**, *17*, 1001.
(52) Wu, T. X.; Liu, G. M.; Zhao, J. C.; Hidaka, H.; Serpone, N. *J. Phys. Chem. B* **1998**, *102*, 5845.
(53) Wu, J. M.; Hang, B.; Zeng, Y. H. *Thin Solid Films* **2006**, *497*, 292.
(54) Ohno, T.; Sarukawa, K.; Matsumura, M. *J. Phys. Chem. B* **2001**, *105*, 2417.